Author's Accepted Manuscript

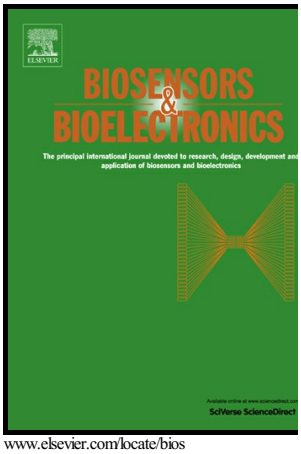


# A High sensitive electrochemical aptasensor for the determination of $VEGF_{165}$ in serum of lung Cancer patient

Mahmoud Amouzadeh Tabrizi, Mojtaba Shamsipur, Leila Farzin

www.elsevier.com/locate/bios

PII: S0956-5663(15)30281-5
DOI: http://dx.doi.org/10.1016/j.bios.2015.07.032
Reference: BIOS7850

To appear in: *Biosensors and Bioelectronic*

Received date: 13 May 2015
Revised date: 2 July 2015
Accepted date: 15 July 2015

Cite this article as: Mahmoud Amouzadeh Tabrizi, Mojtaba Shamsipur and Leila Farzin, A High sensitive electrochemical aptasensor for the determination o $VEGF_{165}$ in serum of lung Cancer patient, *Biosensors and Bioelectronic* http://dx.doi.org/10.1016/j.bios.2015.07.032

This is a PDF file of an unedited manuscript that has been accepted fo publication. As a service to our customers we are providing this early version o the manuscript. The manuscript will undergo copyediting, typesetting, an review of the resulting galley proof before it is published in its final citable form Please note that during the production process errors may be discovered whic could affect the content, and all legal disclaimers that apply to the journal pertain

ACCEPTED MANUSCRIPT

# A high sensitive electrochemical aptasensor for the determination of $VEGF_{165}$ in serum of lung cancer patient

Mahmoud Amouzadeh Tabrizi*[a,b], Mojtaba Shamsipur * [a], Leila Farzin[c]

[a]*Department of Chemistry, Razi University, Kermanshah, Iran.*

[b]*Department of Chemistry, Bonab Research Center, BNRC, NSTRI, P.O. Box 56515-196, Bonab, East Azarbayjan, Iran.*

[c]*Department o f Analytical Chemistry, School of Chemistry, College of Science, University of Tehran, Tehran, Iran.*

*Corresponding authors: Tel/Fax: (+98) 831-4274580,

E-mail: mahmoud.tabizi@gmail.com; mshamsipur@yahoo.com

Accepted manuscript

ACCEPTED MANUSCRIPT

**Abstract**

Herein, a label free electrochemical aptasensor based on ordered mesoporous carbon-gold nanocomposite modified screen printed electrode has been fabricated for the detection of vascular endothelial growth factor ($VEGF_{165}$) as a tumor marker. The electrochemical behavior of prepared biosensor was investigated by cyclic voltammetry and electrochemical impedance spectroscopy. The principle of operation of the proposed aptasensor is based on the changes in the interfacial properties of the electrode due to interaction of the immobilized anti$VEGF_{165}$ aptamer at the electrode surface with $VEGF_{165}$ tumor marker in the sample solution, which results in a change in the interfacial charge transfer resistance as detected by electrochemical impedance spectroscopy. The calibration curve for $VEGF_{165}$ determination was linear over 10.0 to 300.0 pg $mL^{-1}$ with a limit of detection ($3\sigma/S$) of 1.0 pg $mL^{-1}$. The prepared aptasensor exhibited high sensitivity and good selectivity and reproducibility. The aptasensor was successfully applied to the determination of $VEGF_{165}$ in serum sample of a lung cancer patent.

***Keywords:*** Aptasensor; Ordered mesoporous carbon-$Au_{nano}$ composite; $VEGF_{165}$ tumor marker; Label free; Lung cancer

Accepted manuscript

## 1. Introduction

Lung cancer is the second most common cancer after breast cancer and it is by far the leading cause of cancer death for humans (Jemal et al. 2011). Lung cancer accounts for about 13 percent of all new cancers. Worldwide, nearly 1.59 million people were estimated to have died from lung cancer in 2012. The National Institute of Health estimated that the economic cost of lung cancer

ACCEPTED MANUSCRIPT

was about $12.1 billion in this year (Cancer Research UK. 2014). The cases of lung cancer are due to long-term exposure to tobacco smoke (80-90%), radon gas (9-15%), occupational (10%) and outdoor air pollution (1-2%). Hence, it is necessary to develop a sensitive, selective and cost-effective method for the detection of lung cancer disease due to its public health and economic importance.

One of the most effective ways to detect lung cancer is determination of Vascular Endothelial Growth Factor ($VEGF_{165}$) level in human serum samples (A. Abdallah et al. 2014; Amel.Hashim 2015; Acton 2012; Dieter and Norbert 2007). $VEGF_{165}$ is a tumor marker that is produced either by tumor cells itself or by the body in response to the tumor cells in lung cancer patients. Up to now, various analytical methods have been reported in the literature for the determination of $VEGF_{165}$, such as optical methods (Freeman et al. 2012; Gohring et al. 2010; Kopra et al. 2014; M.A.A-Ameen and G.Ghosh 2013; Wang et al. 2014a; Wang et al. 2014; Al-Ameen and Ghosh 2013; Cho et al. 2012; Kopra et al. 2014; Urmann et al. 2015), piezoelectric micro cantilever (Capobianco et al. 2011), field-effect transistor (FET) (Lee et al. 2009; Kwona et al. 2010; O.S.Kwon et al. 2012; Chen et al. 2014a) surface plasmon resonance (SPR) (Liu et al. 2012; Uludag and Tothill 2012; Y.Li et al. 2007; Chen et al. 2014b), quartz crystal microbalance (QCM) (Cabric et al. 2010; Uludag and Tothill 2012), surface-enhanced Raman scattering (SERS) (Ko et al. 2013; Zhao et al. 2015), enzyme-linked immunosorbent assay (ELISA) (Hsu et al. 2015; Yip-Schneider et al.) and electrochemical aptasensors (Li et al. 2007; Lin et al. 2015; Lv et al. 2013; May et al. 2005; Sassolas et al. 2009; Wang et al. 2014b; Zhao et al. 2011). Among these methods, the electrochemical aptasensors are especially promising because of its low cost, selectivity, feasibility of quantification and sensitivity (Luo and Davis 2013; Wu and Qu 2015). Generally, the electrochemical aptasensors divided in two methods “labled” (Wang et

Accepted manuscript

ACCEPTED MANUSCRIPT

al. 2014b) and "label-free" (Chen et al. 2013) aptasensors. While, the label-free aptasensors have certain advantages such as low cost and high stability, compared to labeled aptasensors.

To the best of our knowledge, the use of ordered mesoporous carbon-gold nanocomposite (OMC-$Au_{nano}$) for immobilization of aptamer and its application to fabrication of a label-free electrochemical aptasensor for the detection of $VGEF_{165}$ tumor marker has not yet been reported. The prepared aptasensor exhibited high sensitivity, lower detection limit and high stability for $VEGF_{165}$ sensing.

## 2. Experimental

### 2.1. Chemicals

All chemicals were of analytical reagent grade and used without further purification. Potassium dihydrogen phosphate ($KH_2PO_4$), potassium hydroxide (KOH), potassium chloride (KCl), hydrochloric acid (HCl), potassium hexacyanoferrate(III) ($K_3[Fe(CN)_6]$) and potassium hexacyanoferrate(II) ($K_4[Fe(CN)_6]$) were obtained from Merck (Darmstadt, Germany). Rose water (12 mg natural essence per 100 mL,12%, Rabee Golab, Iran) was obtained from a local market. Vascular endothelial growth factor ($VEGF_{165}$) tumor marker and Anti-$VGEF_{165}$ DNA aptamer were obtained from Invitrogen$^{TM}$ (USA). The aptamer was modified at the 5′-terminus with an SH group and its sequence was as follows:

5′-SH-TTTCCCGTCTTCCAGACAAGAGTGCAGGG-3′.

Human serum human immunoglobulin G (HIgG), human serum immunoglobulin A (HIgA) lipase (Lip), lysozyme (Lys) and human serum albumin (HSA) were obtained from Medical Biology Research Center, Kermanshah University of Medical Sciences, Kermanshah, Iran. All

Accepted manuscript

ACCEPTED MANUSCRIPT

samples were prepared with 0.1 M phosphate buffer solution (PBS, pH=7.4) and stored at 4 $^{\circ}$C before use. Ultrapure water was obtained from a Mill-Q water purification system.

### 2.2. Apparatus

The cyclic voltammetry (CV) and electrochemical impedance spectroscopy (EIS) studies were performed with a model PGSTAT 302N electrochemical workstation (Autolab, Netherlands). The commercial screen printed electrode (SPE) chips were obtained from DrobSens Technology Ltd., Spain. The chips were fabricated by screen-printing technology and designed as system with three electrodes containing carbon working, carbon counter and Ag|AgCl reference electrodes. The impedance spectra were recorded within the range of 100 kHz-0.1 Hz at the formal potential of $K_3Fe(CN)_6/K_4Fe(CN)_6$ ($[Fe(CN)_6^{3-/4-}]$) (1:1) mixture as a redox probe. The amplitude of the alternate voltage was 5 mV. Transmission electron microscopy (TEM) measurements were made on a Hitachi H-8100 microscope with an accelerating voltage of 200 kV. Scanning electron microscopy (SEM) was performed with a Philips instrument (model XL-30, Eindhoven, The Netherlands). Atomic force microscopy (AFM) was conducted with a DME DualScope Scanner DS 95-200. Ultraviolet–visible (UV–vis) absorption spectra were recorded using a single beam Pharmacia UV–vis spectrophotometer (Ultro-spec, model 4000).

Accepted manuscript

### 2.3 Syntheses of OMC and Au nanoparticles

OMC was prepared based on the method reported previously by the use of mesoporous silica material (SBA-15) as template and glucose as carbon source (Jun et al. 2000). Briefly, 1 g SBA-15 silica was first dispersed into 5 g distilled water containing 1.25 g glucose and 0.14 g $H_2SO_4$

ACCEPTED MANUSCRIPT

and stirred for 1 h. Then, the glucose was infiltrated into the channels of SBA-15 silica adequately in a vacuum of 0.1 M Pa for 3 h. The obtained mixture was placed in a drying oven for 6 h at 373 K, and subsequently in 433 K for 6 h. The sample turned dark brown after above treatment. The obtained dark brown sample was completely carbonized by pyrolysis at 1173 K under $N_2$ flow for 3h. Finally the silica template was removed with 5wt% hydrofluoric acid at room temperature to remove the silica template. The product, OMC, was then washed with ultrapure water. The neutral suspension of the filtrate in water was centrifuged at 5000 rpm for 10 min and then the filtrate was re-dispersed in water and centrifuged several times.

Also, the green synthesis process of gold nanoparticles ($Au_{nano}$) was similar as reported previously (Amouzadeh Tabrizi and Varkani 2014). Briefly, 10 mL of rose water and 100 µL $NaAuCl_4$ (0.01 mM) were added into 90.0 mL double distilled water, and the solution was mixed by ultrasonication for 30 min. The mixture was transferred into a reflux apparatus and reacted at 95 °C for 5 h. During this process, the color of the solution changed to red. Based on previous report (Amouzadeh Tabrizi and Varkani 2014), the phenolic compounds in rose water can oxidized to quinine form at 95 °C and release two electrons. These electrons convert the $Au^{3+}$ to $Au_{nano}$.

Accepted manuscript

### 2.4. Fabrication of SPE/OMC-$Au_{nano}$/aptamer

2 mg of OMC was dissolved in 1 mL of isopropanol alcohol and then added to 1 mL $Au_{nano}$ solution. A homogenous solution was obtained after 12 h stirring. Then, 6.0 µL of OMC–$Au_{nano}$ composites were dropped onto the working electrode surface of SPE and allowed to dry at ambient temperature. Subsequently, the SPE was then washed carefully with PBS and immediately immersed in a probe DNA solution (10 µM, 0.05 PBS of pH 7.4) for 24 h. Finally,

ACCEPTED MANUSCRIPT

the electrode (denoted as SPE/OMC-$Au_{nano}$/aptamer) was thoroughly rinsed with deionized ultrafiltered water, dried in air and stored at 4 °C in 0.1 M PBS of pH 7.0 when not in use. During this process, the thiolateded aptamer was covalently attached to the gold nanoparticles of OMC-$Au_{nano}$ composite. After rinsing with 0.1 M PBS buffer, 20 µL of a fixed concentration of $VGEF_{165}$ was dropped onto the surface of SPE/OMC-$Au_{nano}$/aptamer to react for 40 min. After that, the electrode was rinsed three times with water to remove the non-hybridized target. The fabricated aptasensor was stored at 4 °C in refrigerator when not in use. The schematic re-presentation for the fabrication of proposed sensor and the sensing mechanism is shown in Scheme 1.

**<Scheme.1 will be positioned here>**

## 3. Results and discussion

### 3.1. Characterization of the OMC and gold nanoparticles

The SEM images of OMC (A) and Au nanoparticles (B) are shown in Fig.1. The prepared $Au_{nano}$ was also characterized by AFM, TEM and UV-vis spectroscopy (see Fig. S1, Supporting information). The TEM (Fig S.1A) and AFM (Fig S.1B) images showed relatively spherical shape nanoparticles formed with an average diameter 27.4±0.07 nm. The UV-vis absorption spectrophotometry of the prepared $Au_{nano}$ solution is also shown in Fig S.1C. The obtained $Au_{nano}$ displayed an absorption peak at about 530 nm, the characteristic surface plasmon resonance (SPR) band for $Au_{nano}$ (Kasthuri and Rajendiran 2009).

**<Fig.1 will be positioned here>**

Accepted manuscript

ACCEPTED MANUSCRIPT

### 3.2. Electrochemical properties of the electrodes

EIS and CV have been used to characterize the interface properties of surface-modified electrodes. The typical impedance spectrum (presented in the form of the Nyquist plot) includes a semicircle portion at higher frequencies corresponding to the electron-transfer-limited process and a linear part at lower frequency range representing the diffusion limited process (Randviir and Banks 2013). The semicircle diameter in the impedance spectrum equals the charge-transfer resistance ($R_{ct}$). This resistance controls the electron-transfer kinetics of the redox probe at the electrode interface. The impedance measurements were performed in the presence of a 5.0 mM $K_3Fe(CN)_6/K_4Fe(CN)_6$ (1:1) mixture as a redox probe, containing 0.1 M KCl, using an alternating current voltage of 5 mV. The impedance measurements were performed at a bias potential of 0.22 V (vs. Ag|AgCl) obtained from the formal potential of $[Fe(CN)_6^{3-/4-}]$ by CV (Deng et al. 2009; Ocaña et al. 2014). Fig. 2A displays the EIS behavior of $[Fe(CN)_6^{3-/4-}]$ on the SPE (a), SPE/OMC-$Au_{nano}$ (b) and SPE/OMC-$Au_{nano}$/aptamer (c) and SPE/OMC-$Au_{nano}$/aptamer/$VEGF_{165}$ (d). This figure shows that the Nyquist diameter ($R_{ct}$= 58.0 Ω) of SPE/OMC-$Au_{nano}$ is much lower than this observed for SPE ($R_{ct}$= 320.0 Ω), suggesting that OMC-$Au_{nano}$ facilitates the rate of electron transfer. After immobilization of the anti-$VEGF_{165}$ aptamer, the value of $R_{ct}$ increased from 58.0 to 435.0 Ω due to the strong electrostatic repulsion interaction between anti-$VEGF_{165}$ aptamer and $[Fe(CN)_6^{3-/4-}]$. After the incubation of $VEGF_{165}$ tumor marker with anti-$VEGF_{165}$ aptamer, the $R_{ct}$ increased to 772.0 Ω. The reasonable explanation is that the incubation of anti-aptamer with tumor marker led to a mass-transfer blocking barrier for $[Fe(CN)_6^{3-/4-}]$ and hindering the access of this redox probe toward the electrode surface. Therefore, the charge transfer resistance of the aptasensor increased accordingly (Ocaña et al. 2014; Rivas et al. 2015). The model of circuit is inserted in Fig. 2A, in

ACCEPTED MANUSCRIPT

which $R_s$, $Z_W$, $R_{ct}$ and $C_{dl}$ represent the solution resistance, the Warburg diffusion resistance, the charge-transfer resistance and the double layer capacitance, respectively. Also, Fig. 2B displays the CV behavior of $[Fe(CN)_6^{3-/4-}]$ on the SPE (a), SPE/OMC-$Au_{nano}$ (b) and SPE/OMC-$Au_{nano}$/aptamer (c) and SPE/OMC-$Au_{nano}$/aptamer/$VEGF_{165}$ (d). This figure shows that the peak current intensity on SPE/OMC-$Au_{nano}$ was higher than that observed for the SPE. This result demonstrated that OMC-$Au_{nano}$ nanocomposites provide higher electron conduction pathways. But when the probe anti-$VEGF_{165}$ aptamer was assembled on the surface of the SPE/OMC-$Au_{nano}$ (b), the peak current was largely decreased. Then, the incubation of anti-$VEGF_{165}$ aptamer with $VEGF_{165}$ tumor marker, the peak current continuously decreased (c). These results were consistent with the EIS results.

**<Fig.2 will be positioned here>**

### 3.3. Impedimetric detection of $VEGF_{165}$ tumor marker

The influence of amount of OMC-$Au_{nano}$ over the range of 3.0 µL to 8.0 µL of composite on the response of aptasensor to 150 pg $mL^{-1}$ of $VEGF_{165}$ was studied (Fig. 3A). As shown in this figure, with increasing amount of OMC-$Au_{nano}$ composite from, the response of aptamer increased and reached a maximum at 6.0 µL. The effect of incubation time of $VEGF_{165}$ (100 pM) on the sensor response was also investigated (Fig. 3B). As seen, the $\Delta R_{ct}$ increased rapidly with increasing incubation time up to 40 min, and remained unchanged at longer incubation times, suggesting that the formation of $VEGF_{165}$-aptamer aggregate at the electrode surface has reached to a saturation level. Therefore, 6.0 µL of OMC-$Au_{nano}$ composite solution and an incubation time of 40 min have been chosen as the optimum condition for the fabrication of the $VEGF_{165}$ aptasensor throughout this work.

Accepted manuscript

ACCEPTED MANUSCRIPT

The analytical calibration was performed by EIS (Fig.3C). It can be seen that, after the incubation of anti-$VEGF_{165}$ aptamer with $VEGF_{165}$ tumor marker, the $R_{ct}$ increases with the increasing $VEGF_{165}$ concentration due to mass-transfer limiting of $[Fe(CN)_6^{3-/4-}]$ to the electrode surface. The $\Delta R_{ct}$ increases with increasing $VEGF_{165}$ concentration from 10.0 to 300.0 pg $mL^{-1}$ with a limit of detection of 1.0 pg $mL^{-1}$ ($3\sigma/S$) (Fig. 3D). The linear regression equation obtained $\Delta R_{ct}$ ($\Omega$) =4.935 $C_{[VEGF165]}$ (pg $mL^{-1}$) + 95.988 (Eq:1)

**<Fig.3 will be positioned here>**

To evaluate the selectivity of the proposed aptasensor, some biomolecules such as HIgG, HIgA, Lip, Lys and HSA were used as the interference to evaluate the specificity and the results are shown in Fig.4. In this process, the interfering effect of each one of the biomolecules was studied by new apasensors. The concentrations of the interfering substances were 100.0 times that of $VEGF_{165}$ (100.0 pg $mL^{-1}$). As it can be clearly seen from Fig. 4, the presence of other proteins than $VEGF_{165}$ at 100 times excess has negligible effect on the main signal. For example, HIgG, shows only about 0.5% error in detection of $VEGF_{165}$. This was probably due to the loosely physical adsorption of HIgG on the porous structure of surface modified electrode that it can be washed away by carefully rising with PBS. As indicated, the proposed aptasensor possesses a high selectivity for $VEGF_{165}$, which resulted from high affinity and specificity of the aptasensors towards the presence of specific nucleic acid sequences in their structures that can bind to a favorite target (Berezovski et al. 2006; Berezovski et al. 2008).

**<Fig.4 will be positioned here>**

The intra and inter reproducibility of proposed aptasensor were also considered. The intra reproducibility was estimated by measurements of 150 pg $mL^{-1}$ of $VEGF_{165}$ with the same sensor. The relative standard deviation (RSD) for a series of five experiments was achieved to be

ACCEPTED MANUSCRIPT

5.4%. The inter reproducibility was also evaluated by using SPE/OMC-$Au_{nano}$/aptamer for determinations of 150 pg $mL^{-1}$ of $VEGF_{165}$ with five different sensors. The RSD was calculated to be 6.9%.

The proposed aptasensor was employed for the determination of $VEGF_{165}$ in lung cancer of human blood serum to examine its applicability for real sample analysis. The human serum sample was prepared by local hospital laboratory based on previous report (Proimmune, the Oxford Science Park, 2009). Briefly, 5 mL of freshly human blood was transferred into a tube and it was keept at room temperature for 20 minutes. After that, the human blood was centrifuged for 10 min at 3000.0 rpm. Finally, a part of above solution was separated and divided into small tubes. The prepared human serum samples were then stored at -80 °C until use.

Then, a 400 µL of lung cancer of human blood serum was mixed with 3.6 mL solution containing of 5 mM $[Fe(CN)_6^{3-/4-}]$ and 0.1 M KCl (pH=7.4) and was then analyzed using EIS method. The concentration of $VEGF_{165}$ in serum of lung cancer patient was determined to be 712.2 pg $mL^{-1}$. The recovery of the analysis was about 97.1%, considering the value determined by a standard ELISA in local hospital (733.5 pg $mL^{-1}$). The study protocol was approved by the Medical Ethics Committee of Kermanshah University of Medical Sciences, Kermanshah, Iran (Arkan et al. 2014).

The comparison of the analytical performance of the proposed $VEGF_{165}$ aptasensor with other electrochemical aptasensors are also summarized in Table 1.

**<Table 1 will be positioned here>**

It can be seen that the proposed aptasensor exhibited high analytical performance in terms of sensitivity, selectivity, reproducibility and low detection limit.

Accepted manuscript

ACCEPTED MANUSCRIPT

## 4. Conclusions

In summary, a novel and ultrasensitive label-free electrochemical aptasensor base on immobilization of anti-VEGF aptamer on the surface of SPE/OMC-$Au_{nano}$ has been developed to detect of $VEGF_{165}$ tumor marker. The analytical results obtained using CV and EIS techniques. EIS technique revealed that there existed a good linear relationship between peak current with the concentration of $VEGF_{165}$ tumor marker in the range of 10.0-300.0 pg $mL^{-1}$ and the detection limit of 1.0 pg $mL^{-1}$.The proposed aptasensor displayed also a good selectivity, sensitivity and reproducibility. This aptasensor was used for the determination of $VEGF_{165}$ in serum sample of lung cancer patient.

**Acknowledgements**

The authors thank the Research Council of Razi University (Kermanshah, Iran) and Iran National Elites Foundation (INEF) for the support of this work. Also, the assistance of Dr. Elham. Arkan from Kermanshah University of Medical Sciences is gratefully acknowledged.

**Supporting Information Available**:

Supplementary data associated with this article can be found in the online version.

Accepted manuscript

## References

A. Abdallah, M.Belal, Bastawisy, A.E., R.Gaafar, 2014. Oncol. Lett. 7, 2121–2129.

Acton, Q.A., 2012. Angiostatic Proteins: Advances in Research and Application. 2012. Scholarly Paper, 1 ed. Scholarly Editions.

Al-Ameen, M.A., Ghosh, G., 2013. Biosens. Bioelectron. 49, 105–110.

Amouzadeh Tabrizi, M., Varkani, J.N, 2014. Sens. Actuators B: Chem. 202, 475–482.

ACCEPTED MANUSCRIPT

E. Arkan, R. Saber, Z. Karimi, A. Mostafaiee, M. Shamsipur, 2014. J. Pharm. Biomed. Anal, 92, 74–81.

Berezovski, M., Musheev, M., Drabovich, A., Krylov, S.N., 2006. J. Am. Chem. Soc.128, 1410–1411.

Berezovski, M.V., Lechmann, M., Musheev, M.U., Mak, T.W., Krylov, S.N., 2008. J. Am. Chem. Soc.130, 9137–9143.

Cabric, S., Sanchez, J., Johansson, U., Larsson, R., Nilsson, B., Korsgren, O., Magnusson, P.U., 2010. Tissue Eng Part A. 16, 961–970.

Capobianco, J.A., Shih, W.Y., Adams, G.P., Shih, W.-H., 2011. Sens. Actuators B: Chem. 160, 349–356.

Chen, H.-C., Qiu, J.-T., Yang, F.-L., Liu, Y.-C., Chen, M.-C., Tsai, R.-Y., Yang, H.-W., Lin, C.-Y., Lin, C.-C., Wu, T.-S., Tu, Y-.M., Xiao, M.-C., Ho, C.-H., Huang, C.-C., Lai, C.-S., Hua, M.-Y., 2014a. Anal. Chem. 86, 9450–9443.

Chen, J.R., Jiao, X.X., Luo, H.Q., Li, N.B., 2013. J. Mater. Chem. B. 1, 861–864.

Chen, H., Hou, Y., Qi, F., Zhang, J., Koh, K., Shen, Z., Li, G., 2014b. Biosens. Bioelectron. 61, 83–87.

Cheng, W., Ding, S., Li, Q., Yu, T., Yin, Y., Ju, H., Ren, G., 2012. Biosens. Bioelectron. 36, 12–17.

Cho, H., Yeh, E.-C., Sinha, R., Laurence, T.A., Bearinger, J.P., Lee, L.P., 2012. ACS Nano 6, 7607–7614.

Dieter, M., Norbert, F., 2007. Tumor Angiogenesis :Basic Mechanisms and Cancer Therapy, 1 ed. Springer Science & Business Media.

Accepted manuscript

ACCEPTED MANUSCRIPT

Deng, C., Chen, J., Nie, Z., Wang, M., Chu, X., Chen, X., Xiao, X., Lei, C., Yao, S., 2009. Anal. Chem. 81, 739-745.

Freeman, R., Girsh, J., Fang-ju Jou, A., Ho, J.-a.A., Hug, T., Dernedde, J., Willner, I., 2012. Anal. Chem. 84, 6192–6198.

Gohring, J.T., Dale, P.S., Fan, X., 2010. Sens. Actuators B: Chem. 146, 226–230.

Hashim, A., 2015. Serum VEGF165 and HGF in Egyptian Patients with Lung and Pleural Cancers, 1 ed. Scientific Research Publishing.

Govorukhina, N.I., Keizer-Gunnink, A., van der Zee, A.G.J., de Jong, S., de Bruijn, H.W.A., Bischoff, R., 2003. J Chromatogr A.1009, 171-178

H-S, Lee., K-S, Kim, C-J, Kim, SK, Hahan, M-H, Jo., 2009. Biosens Bioelectron. 24, 1801–1805.

Hsu, M.-Y., Chen, S.-J., Chen, K.-H., Hung, Y.-C., Tsai, H.-Y., Cheng, C.-M., 2015. Lab on a Chip, 15, 2357–2363.

Jemal, A., Bray, F., Center, M.M., Ferlay, J., Ward, E., Forman, D., 2011. CA Cancer J Clin. 61, 69–90.

Jun, S., Joo, S.H., Ryoo, R., Kruk, M., Jaroniec, M., Liu, Z., Ohsuna, T., Terasaki, O., 2000. J. Am. Chem. Soc. 122, 10712–10713.

Kasthuri, J., Rajendiran, N., 2009. Colloids Surf. B: Biointerf. 73, 387–393.

Ko, J., Lee, S., Lee, E.K., Chang, S.-I., Chen, L., Yoon, S.-Y., Choo, J., 2013. PCCP. 15, 5379–5385.

Kopra, K., Syrjanpaa, M., Hanninen, P., Harma, H., 2014. Analyst 139, 2016–2023.

Accepted manuscript

ACCEPTED MANUSCRIPT

Kwona, O.S., Hong, T.-J., Kim, S.K., Jeong, J.-H., Hahn, J.-S., Jang, J., 2010. Biosens. Bioelectron. 25, 1307–1312.

Lee, H.S., Kim, K.S., Kim, C.J., Hahn, S.K., Jo, M.H., 2009. Biosens. Bioelectron. 24, 1801–1805.

Li, B., Du, Y., Wei, H., Dong, S., 2007. Reusable, Chem. Commun. 3780–3782.

Lin, C.-W., Wei, K.-C., Liao, S.-S., Huang, C.-Y., Sun, C.-L., Wu, P.-J., Lu, Y.-J., Yang, H.-W., Ma, C.-C.M., 2015. Biosens. Bioelectron. 67, 431–437.

Liu, C., Lei, T., Ino, K., Matsue, T., Tao, N., Li, C.-Z., 2012. Chem. Commun. 48, 10389–10391.

Luo, X., Davis, J.J., 2013. Chem. Soc. Rev.42, 5944–5962.

Lv, Z., Wang, K., Zhang, X., 2013. J Immunoassay Immunochem. 35, 233–240.

M.A.A-Ameen, G.Ghosh, 2013. Biosens. Bioelectron. 49, 105–110.

May, K.L., Vogt, A., Bachas, L., Anderson, K., 2005. Anal Bioanal Chem 382, 1010–1016.

Ocaña, C., Arcay, E., del Valle, M., 2014. Sens. Actuators B: Chem. 191, 860–865.

O.S.Kwon, S.J.Park, j-Y.Hong, A-R.Han, J.S.Lee, Lee, J.S., J.H.Oh, J.Jang, 2012. ACS Nano. 6, 1486–1493.

Randviir, E.P., Banks, C.E., 2013. Anal. Methods. 5, 1098–1115.

Rivas, L., Mayorga-Martinez, C.C., Quesada-González, D., Zamora-Gálvez, A., de la Escosura-Muñiz, A., Merkoçi, A., 2015. Anal. Chem. 87, 5167–5172.

Sassolas, A., Blum, L.J., Leca-Bouvier, B.D., 2009. Electroanalysis 21, 1237–1250.

Uludag, Y., Tothill, I.E., 2012. Anal. Chem. 84, 5898–5904.

Urmann, K., Walter, J.-G., Scheper, T., Segal, E., 2015. Anal. Chem. 87, 1999–2006.

Wang, S.-E., Huang, Y., Hu, K., Tian, J., Zhao, S., 2014a. Anal. Methods. 6, 62–66.

Wang, X., Jiang, A., Hou, T., Li, F., 2014b. Analyst. 139, 6272–6278.

Accepted manuscript

ACCEPTED MANUSCRIPT

Wu, L., Qu, X., 2015. Chem. Soc. Rev.44, 2963–2997.

Y.Li, J.Lee, H., M.Corn, R., 2007. Anal. Chem. 79, 1082–1088.

Yip-Schneider, M.T., Wu, H., Dumas, R.P., Hancock, B.A., Agaram, N., Radovich, M., Schmidt, C.M., J Am Coll Surg. 218, 608–617.

Zhao, J., He, X., Bo, B., Liu, X., Yin, Y., Li, G., 2012. Biosens. Bioelectron. 34, 249–252.

Zhao, S., Ma, W., Xu, L., Wu, X., Kuang, H., Wang, L., Xu, C., 2015. Biosens. Bioelectron. 68, 593–597.

Zhao, S., Yang, W., Lai, R.Y., 2011. Biosens. Bioelectron. 26, 2442–2447.

**Web References**

http://publications.cancerresearchuk.org/downloads/product/CS_KF_LUNG.pdf.

https://www.proimmune.com/ecommerce/pdf_files/PR31.pdf

Accepted manuscript

ACCEPTED MANUSCRIPT

**Captions of Figures**

**Scheme 1.** The schematic illustration for fabrication and sensing mechanism of proposed aptasensor.

**Fig.1.** SEM images of OMC (A) and Au nanoparticles.

**Fig.2.** (A) Electrochemical impedance spectra and (B) Cyclic voltammograms of (a) SPE, (b) SPE/OMC-$Au_{nano}$, (c) SPE/OMC-$Au_{nano}$/aptamer and (d) SPE/OMC-$Au_{nano}$/aptamer/$VEGF_{165}$ in a solution containing 5.0 mM [$Fe(CN)_6^{3-/4-}$] couple (1:1) and 0.1 M KCl (pH=7.4). The bias potential for EIS is 0.22 V. Inset is the equivalent electric circuit compatible with the Nyquist diagrams. $R_s$: solution resistance, $R_{ct}$: charge transfer resistance, $C_{dl}$: double layer capacitance, $Z_w$: Warburg impedance.

**Fig.3.** (A) Effect of value of OMC-$Au_{nano}$ composite and the incubation time (B) on the response of SPE/OMC-$Au_{nano}$/aptamer to 150.0 pg $mL^{-1}$ of $VEGF_{165}$ in a solution containing 5.0 mM [$Fe(CN)_6^{3-/4-}$] couple (1:1) and 0.1 M KCl (pH=7.4). (C) Electrochemical impedance spectra results for SPE/OMC-$Au_{nano}$/aptamer incubated with different concentrations of $VEGF_{165}$ (0, 10, 50, 100, 150, 200, 250 and 300 from inner to outer with 50 pg $mL^{-1}$ increments). (D) Calibration curve for $\Delta R_{ct}$ versus concentration of $VEGF_{165}$.

**Fig.4.** Selectivity of the proposed aptasensor shown in different $\Delta R_{ct}$ scales (A and B) for $VEGF_{165}$ in presence of 100 times excess of HIgG, HIgA, Lip, Lys and HSA as interfering species. Concentration of $VEGF_{165}$ is 100 pg $mL^{-1}$ and that of the others are 10 ng $mL^{-1}$.

Accepted manuscript

ACCEPTED MANUSCRIPT

**Table 1.** Comparison of the analytical performance of the different $VEGF_{165}$ aptasensors.

| Modified electrode | Electrochemical method | Liner range (pg/mL) | LOD (pg/mL) | Ref. |
|---|---|---|---|---|
| GSPE/MGO- Avastin | DPV | $31.25–2.0\times10^3$ | 31.25 | (Lin et al. 2015) |
| GSPE/aptamer-MB | ACV | 190.0-760.0 | 190.0 | (Zhao et al. 2011) |
| GE/aptamer-FC | SWV | $38.0\times10^3$-$760.0\times10^3$ | $38\times10^3$ | (Zhao et al. 2012) |
| GE/aptamer-Hairpin | DPV | 1.0-$1.0\times10^3$ | 0.82 | (Cheng et al. 2012) |
| SiNW-FETs/aptamer | FET | 100.0-$38.0\times10^3$ | 100.0 | (Lee et al. 2009) |
| GE/aptamer/Hemin | DPV | $38\times10^3$-$11.4\times10^6$ | $38\times10^3$ | (Lv et al. 2013) |
| SPE/OMC-$Au_{nano}$/aptamer | EIS | 10.0-300.0 | 1.0 | This work |

MGO: Magnetic graphene oxide; GSPE: Gold base screen printed electrode; MB: Methylene blue; FC: Ferrocene; DPV: Differential pulse voltammetry; ACV: AC voltammetry; SWV: Square wave voltammetry; FET: Field-effect transistor; CPNTs: Carboxylated polypyrrole nanotubes; SiNW: Si nanowire.

Accepted manuscript

**Figures**

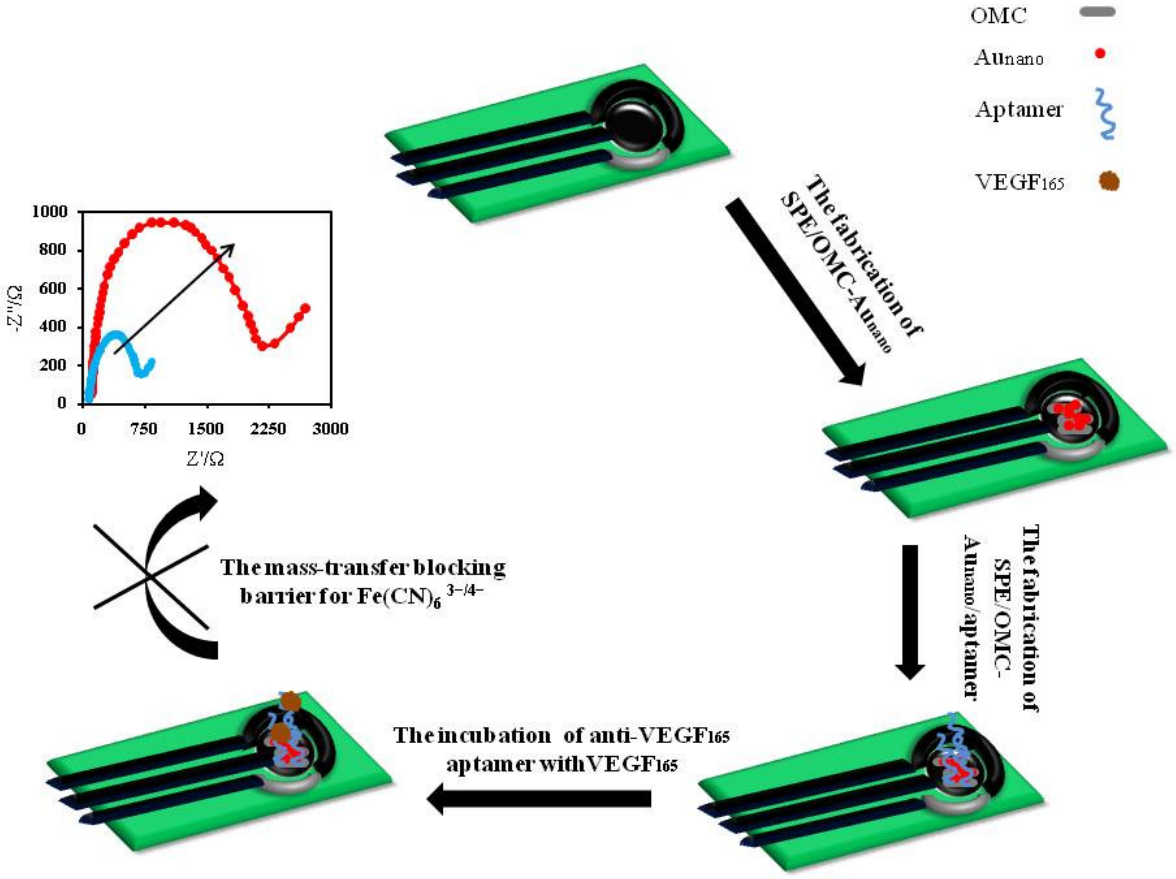


**Scheme 1.**

Accep

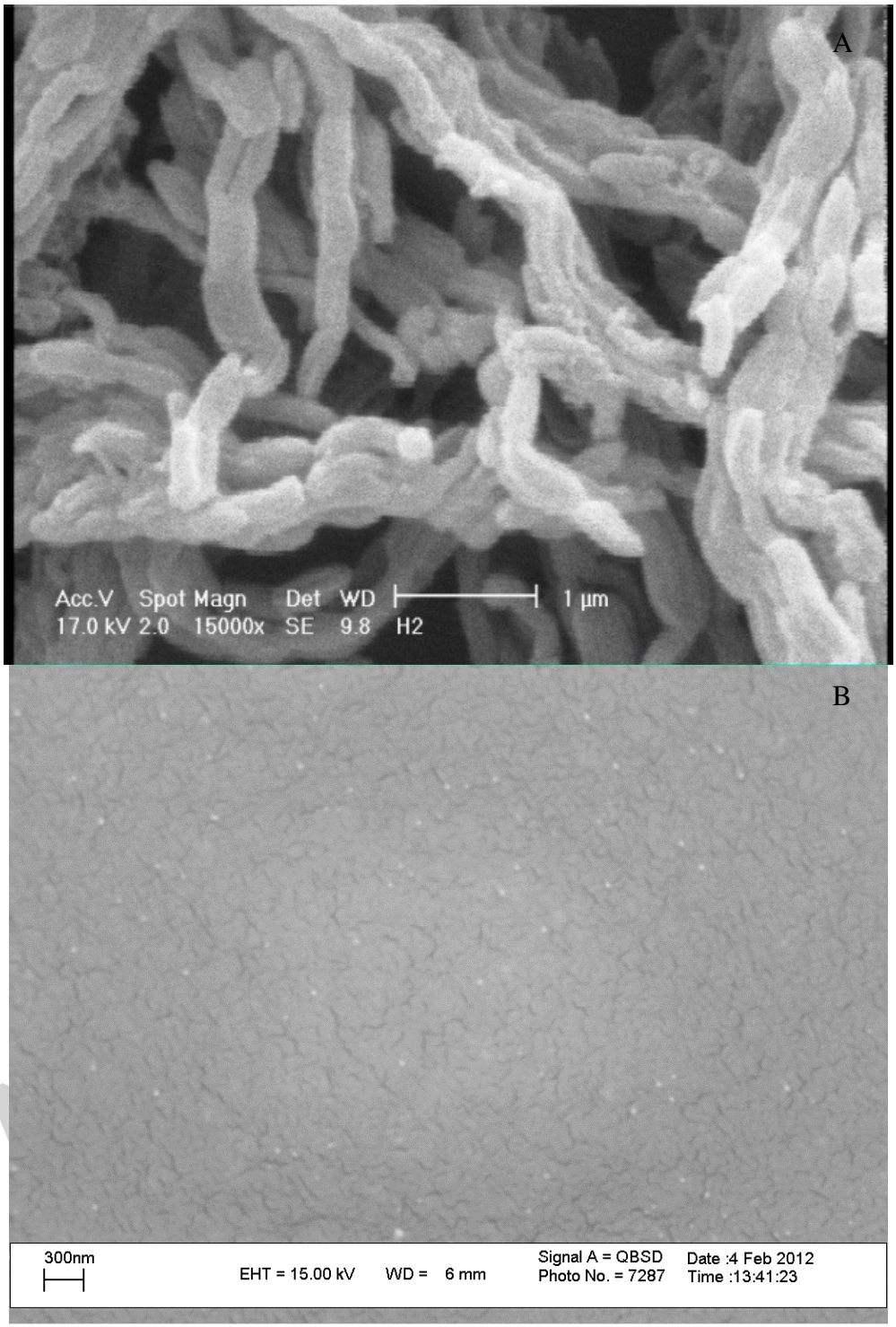
A
Acc.V Spot Magn Det WD 1 µm
17.0 kV 2.0 15000x SE 9.8 H2
B
300nm
EHT = 15.00 kV WD = 6 mm
Signal A = QBSD
Photo No. = 7287
Date :4 Feb 2012
Time :13:41:23

**Fig.1.**

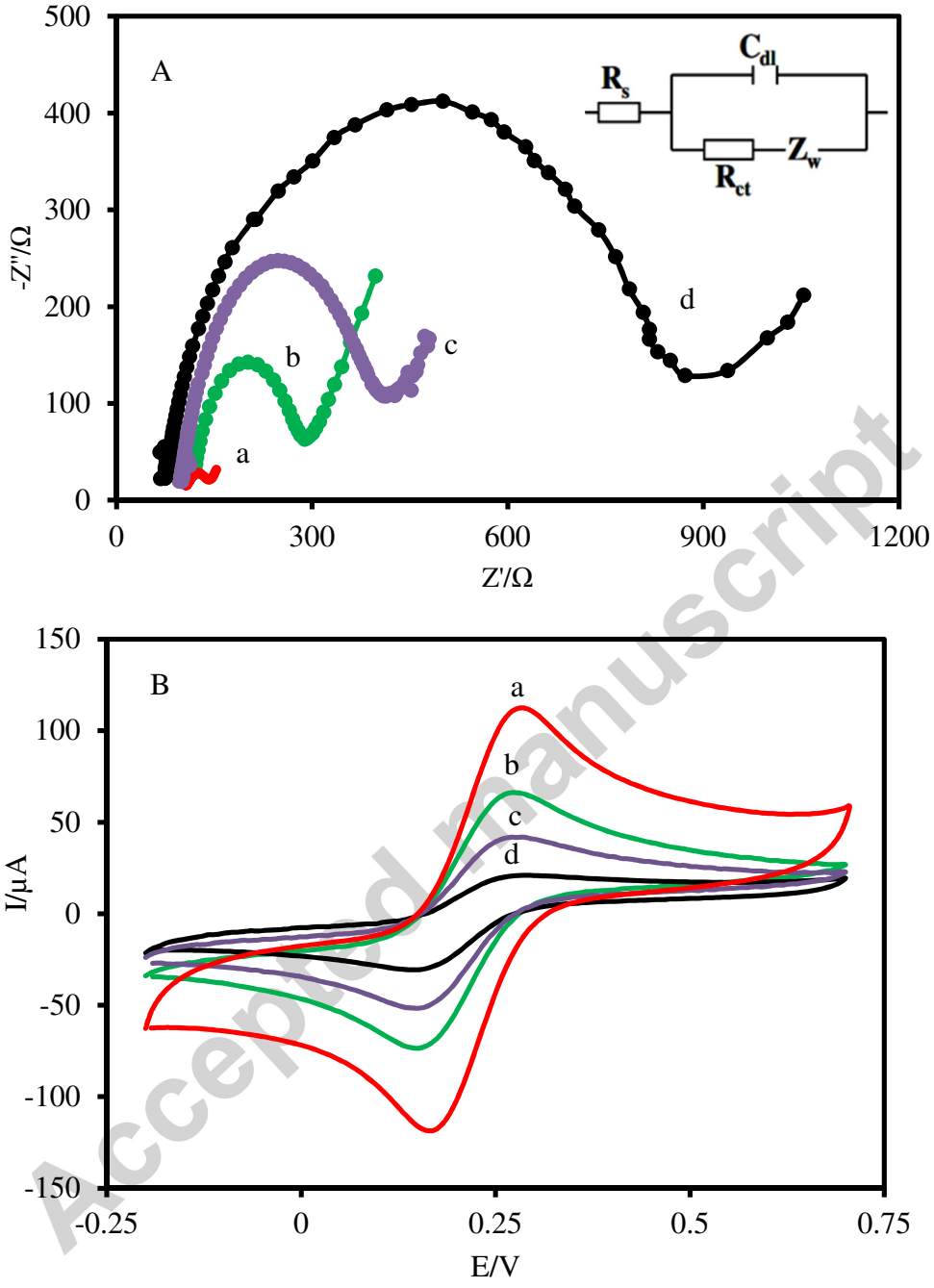


Accepted manuscript

**Fig.2.**

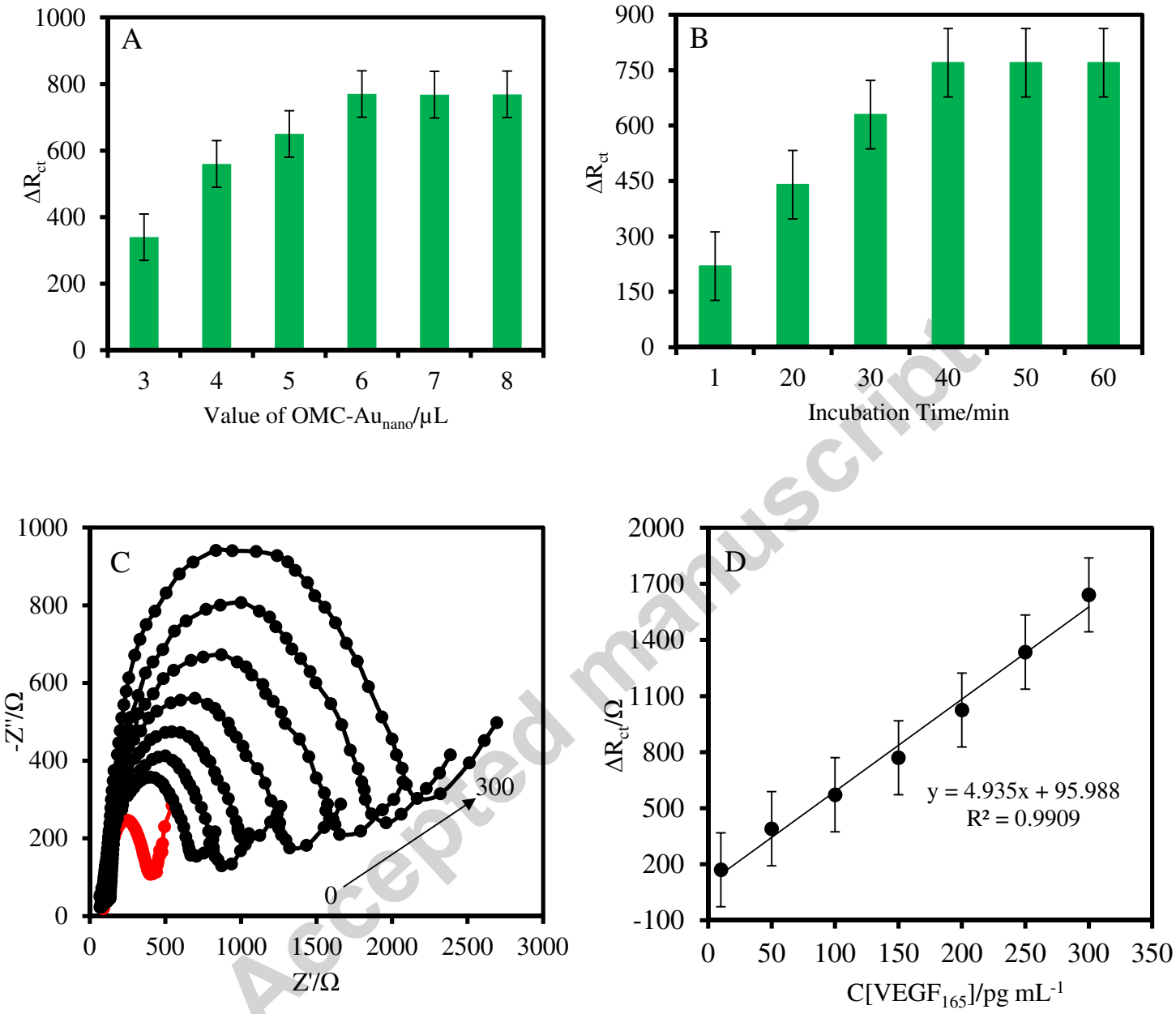


**Fig.3.**

Accepted manuscript

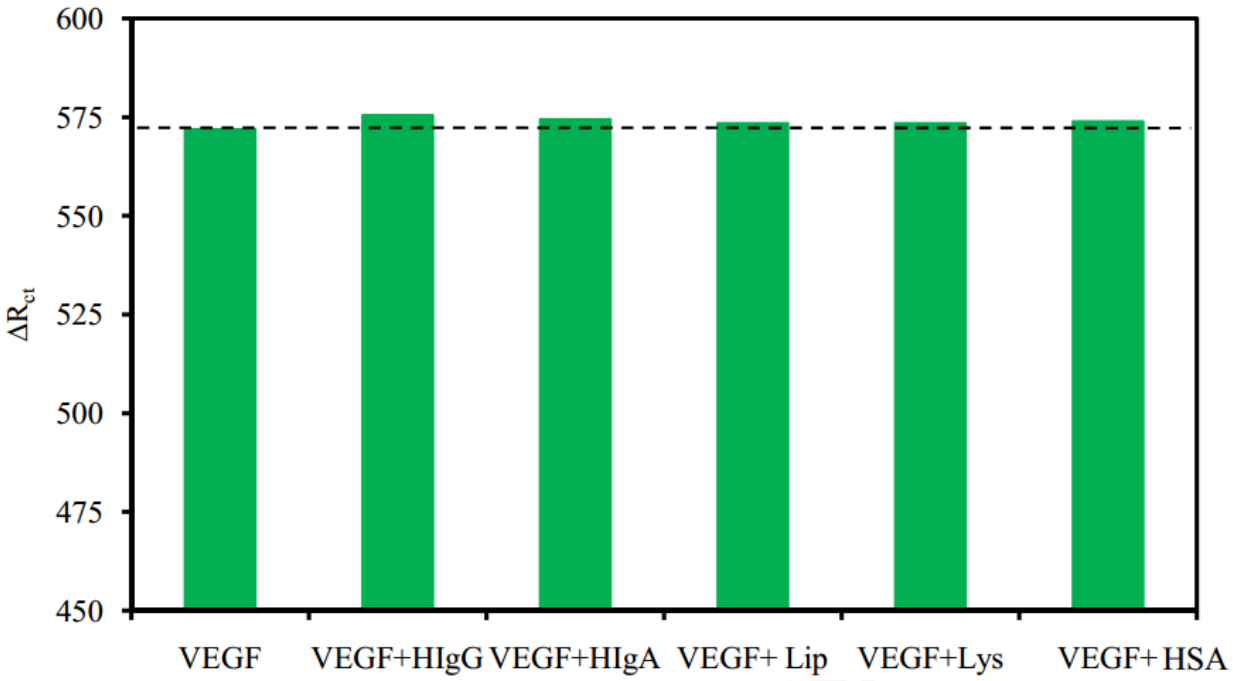


**Fig.4.**

Accepted manuscript

**Highlights**

- An aptasensor for the detection of $VGEF_{165}$ using SPE/OMC-$Au_{nano}$/aptamer has been reported.
- EIS technique was used for the determination of $VGEF_{165}$ tumor marker.
- The determination of $VGE_{F165}$ up to 300 pg $mL^{-1}$ with a limit of detection of 1 pg $mL^{-1}$, respectively.
- This aptasensor was applied for the determination of $VEGF_{165}$ in serum sample of lung cancer patent.